

A Silicon Shallow-Ridge Waveguide Integrated Superconducting Nanowire Single Photon Detector Towards Quantum Photonic Circuits *

Lingjie Yu(俞凌杰)^{1,2†}, Heqing Wang(王河清)^{3,4†}, Hao Li(李浩)³, Zhen Wang(王镇)³,
Yidong Huang(黄翊东)^{1,2}, Lixing You(尤立星)^{3**}, Wei Zhang(张巍)^{1,2**}

¹Beijing National Research Center for Information Science and Technology, Beijing Innovation Center for Future Chips,
Electronic Engineering Department, Tsinghua University, Beijing 100084

²Beijing Academy of Quantum Information Sciences, Beijing 100193

³State Key Laboratory of Functional Materials for Informatics, Shanghai Institute of Microsystem and Information
Technology, Chinese Academy of Sciences, Shanghai 200050

⁴University of Chinese Academy of Sciences, Beijing 100049

(Received 8 May 2019)

A silicon shallow-ridge waveguide integrated superconducting nanowire single photon detector is designed and fabricated. At the bias current of 11.6 μ A, 4% on-chip detection efficiency near 1550 nm wavelength is achieved with the dark count rate of 3 Hz and a timing jitter of 75 ps. This device shows the potential application in the integration of superconducting nanowire single photon detectors with a complex quantum photonic circuit.

PACS: 42.50.-p, 42.82.-m, 74.78.-w

DOI: 10.1088/0256-307X/36/8/084202

In recent decades, technology based on quantum photonics has experienced huge development.^[1–3] The quantum photonic circuit or chip emerges,^[4–8] which meets the demand for system miniaturization, and has the advantage of scalability and stability. Various material platforms such as silicon,^[6,7] silicon nitride,^[5] silica^[4] and III–V materials^[8] have been applied in practice. In these experiments, the function of quantum photonic state manipulation and detection are usually separated into two individual chips. Photons are transmitted between the chips by means of fiber and a micro-nano on-chip structure, such as a grating coupler^[7] and spot-size converter.^[6] The brought-in coupling loss leaves room for improvement. Furthermore, for quantum photonic circuit with multi-outputs, each output port needs to be connected to an individual single photon detection chip. The system scaling up, and the amount of detection chips increases rapidly,^[7] raises the system complexity in practice. The superconducting nanowire single photon detector (SNSPD),^[9] thanks to its excellent performance of high detection efficiency,^[10,11] high detection speed^[12] and low noise level,^[13–15] has attracted wide attention and has been extensively used in quantum photonics. Moreover, the fabrication process of SNSPD is compatible with that of various material platforms for quantum photonic circuits^[16–19] and makes it possible to define the nanowire array on the multi-outputs.^[20] Hence, the integration of SNSPD together with a functional unit for quantum photonic state manipulation is a good idea to reduce the inter-chip loss, to solve the scaling-up problem, and largely to improve the integration level.

A waveguide, the basic role of transmission, can also compose the on-chip devices like a directional coupler, Mach–Zehnder interferometer in a quantum photonic circuit.^[6] Therefore, integrating the waveguide and SNSPD paves the way to the integration of SNSPDs with a complex quantum photonic circuit. During recent years, several remarkable works have been reported, among which different combinations of waveguide material platforms, waveguide types and superconducting nanowire materials have been adopted, such as the GaAs ridge waveguide with NbN superconducting nanowire,^[16] a silicon strip waveguide with NbN superconducting nanowire,^[17] a silicon nitride rib waveguide with NbN superconducting nanowire,^[18] a silicon nitride strip waveguide with NbTiN superconducting nanowire,^[20] and a diamond rib waveguide with NbN superconducting nanowire.^[19] The silicon platform, as an important route for quantum photonic circuit, can realize almost all the quantum state manipulation function and has the potential of large-scale integration.^[6,7,21] Strip and shallow-ridge waveguides, as the two most frequently used ones, have their own pros and cons. A silicon strip waveguide has a smaller bending radius and therefore more integration density.^[22] Meanwhile, the silicon shallow-ridge waveguide has several advantages, such as a compatible fabrication process with the grating coupler, and low transmission loss due to its small overlap between the mode field and the rough side walls of waveguide^[23] arising from the non-ideal fabrication. Therefore, the shallow-ridge waveguide and strip waveguide are complementary on silicon platforms. Hence, the silicon shallow-ridge waveguide

*Supported by the National Key R&D Program of China under Grant Nos 2017YFA0303704 and 2017YFA0304000, the National Natural Science Foundation of China under Grant Nos 61575102, 91750206, 61671438, 61875101 and 61621064, the Beijing Natural Science Foundation under Grant No Z180012, and the Beijing Academy of Quantum Information Sciences under Grant No Y18G26.

[†]Lingjie Yu and Heqing Wang contributed equally to this work.

**Corresponding author. Email: lxyou@mail.sim.ac.cn; zwei@tsinghua.edu.cn

© 2019 Chinese Physical Society and IOP Publishing Ltd

deserves the study on its interaction with superconducting nanowire, which helps in the realization of complex quantum photonic circuits.

In this work, we realize a silicon shallow-ridge waveguide integrated superconducting nanowire single photon detector. The silicon-on-insulator (SOI) platform is chosen to fabricate the shallow-ridge waveguides and the grating couplers. Niobium nitride (NbN), as a well-developed material for single photon detection, is adopted to fabricate the superconducting nanowire. The measurement results show that this device has potential on future quantum photonic circuits with large-scale detector array. Firstly, the absorption of NbN nanowire on the shallow-ridge waveguide is analyzed theoretically, followed by the introduction of the design and fabrication of the device sample in the second part. Then the measurement results of the device performance are shown in the third part and the conclusion is finally given.

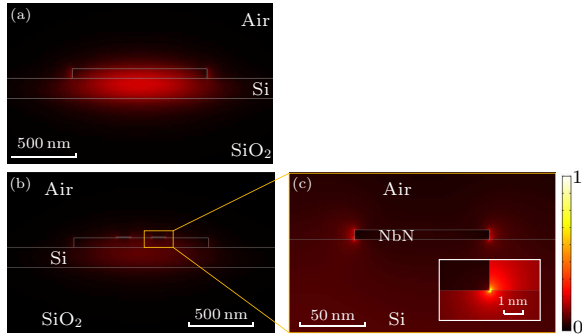


Fig. 1. The fundamental mode profile of a silicon shallow-ridge waveguide without (a) and with (b) the NbN nanowire on top. (c) The enlarged area around the NbN nanowire in (b). The color bar represents the normalized modulus of electric field intensity. Without the NbN nanowire, the electric field is concentrated in the center of the waveguide, while with the NbN nanowire laid on top, the strongest electric field part is in a small area around the nanowire. It leads to strong photon absorption by the NbN nanowire, which contributes to the single photon detection.

Compared to the silicon strip waveguide, the silicon shallow-ridge waveguide has weaker interaction with superconducting nanowire because of the smaller overlap between its mode field and the nanowire. This may lead to a larger superconducting nanowire in length. The absorption ratio is estimated using COMSOL Multiphysics. The fundamental mode of the shallow-ridge waveguide without and with NbN nanowire on top is calculated, and the electric field distributions are shown in Fig. 1. Without the NbN nanowire, the electric field is concentrated in the center of the waveguide (Fig. 1(a)), while with the NbN nanowire laid on top, the strongest electric field part is in a small area around the NbN nanowire (Figs. 1(b), 1(c) and its inset). It leads to strong photon absorption by the NbN nanowire, which contributes to the single photon detection. The effective mode indices are $n_{\text{eff}1} \approx 2.77$ and $n_{\text{eff}2} \approx 2.78 - 0.026i$, respectively.

As a contrast, the effective mode indices of a strip waveguide without and with NbN nanowire on top are $n_{\text{eff}3} \approx 2.39$ and $n_{\text{eff}4} \approx 2.41 - 0.051i$, respectively. The imaginary parts in $n_{\text{eff}2}$ and $n_{\text{eff}4}$ correspond to the absorption of the NbN nanowire in photon propagation. To absorb 99% of photons propagating in this region, the lengths of NbN nanowires on shallow-ridge and strip waveguide are worked out as $21.82 \mu\text{m}$ and $11.03 \mu\text{m}$, respectively. The comparison shows that the shallow-ridge waveguide SNSPD can also absorb light sufficiently, while it needs a longer superconducting nanowire length due to the weaker interaction.

In the design, the chip consists of three main parts: a grating coupler, waveguide and superconducting nanowire. The 220 nm SOI platform is used to fabricate grating couplers and waveguides. The type of shallow-ridge waveguide is chosen because of its low transmission loss and the same 70 nm etching depth with the grating coupler. The width of the shallow-ridge waveguide is set to be $1 \mu\text{m}$. The period and fill factor of the 1D focusing grating coupler are set to be 630 nm and 50%, respectively. With an 8-degree incident angle, the central wavelength of the grating coupler is designed to be 1550 nm. With the focusing configuration, the photons coupled by the grating coupler will converge into the waveguide. The grating coupler coupling the incident photons is set at the center of the chip. In the waveguide structure, a 50:50 Y-junction is used, after which half of the incoming photons are transmitted to the superconducting nanowire for single photon detection, and the remains are transmitted to the other grating coupler for photon loss calibration. The total transmission distance from the first grating coupler to the superconducting nanowire and the second grating coupler are both about $500 \mu\text{m}$. The gap of two grating couplers is set as $250 \mu\text{m}$ to fit the commercial fiber array in calibration. NbN is chosen as the superconducting nanowire material. The width and thickness of superconducting nanowire are set to be 100 nm and 7 nm, respectively. To realize the maximal absorption, the core superconducting nanowire is set as U-shaped and placed right above the waveguide. The transmission distance is set to be $20 \mu\text{m}$. Based on the simulation, about 98% of photons propagating in this region will be absorbed after $20 \mu\text{m}$ propagation forward. Moreover, two on-chip electrical inductances are added to extend the response time to prevent detector latching.^[24]

The fabrication processes of the device are as follows: Firstly, the gold alignment markers are fabricated by the electron-beam evaporation process and lift-off. The thickness of gold markers is 80 nm to guarantee the high contrast for the next alignment. Secondly, the chip is coated by the electron-beam resist ZEP520, and the shallow-ridge waveguides and grating couplers are patterned via the EBL process and etched out by the inductively coupled plasma reactive ion etching (ICP-RIE) process. The depth of etching is precisely controlled at 70 nm. Next, the

electrode is firstly formed by the NbN film using ultra-violet lithography and the lift-off process. Compared with the reactive-ion etching, the silicon waveguide can be protected from being over etched via lift-off. The 7-nm-thick NbN film is deposited by reactive dc magnetron sputtering in an Ar/N₂ gas mixture at a ratio of 30:4 (with a total pressure of 0.273 Pa) and then soaked in acetone for lift-off. Finally, the chip is coated by the electron-beam resist PMMA, patterned into a nanowire structure via electron-beam lithography, and etched via reactive-ion etching in a CF₄ plasma. The structure of the device is shown in Fig. 2(a).

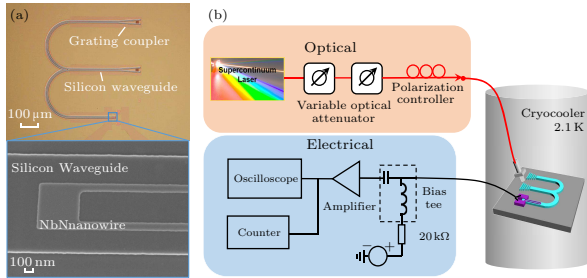


Fig. 2. (a) Optical microscope image of chip sample. Inset: SEM image of detection core area. (b) Schematic view of measurement setup.

The fabricated device is packaged into a copper sample mount. This packaged module is then mounted on the cold head of two-stage Gifford–McMahon cryocooler under the working temperature of 2.1 K. Figure 2(b) shows the whole setup of the measurement with optical and electrical access. The pulsed laser is prepared using a supercontinuum laser (NKT: EXB-3) and an acousto-optic tunable filter (NKT: SuperK SELECT). The laser is then connected in series with two variable attenuators and a polarization controller. With fiber focused with the grating coupler, the light is coupled into the waveguide and absorbed by the NbN nanowire. The power of the light is measured with a power meter (Thorlabs: S154C) and then attenuated to achieve a photon flux of 10^5 photon/s. Error due to the calibration of the laser power is less than 3.5% as given by the power meter, and the laser power fluctuation is less than 1.2%. We apply a bias current and read out the detection signal with a bias tee separating high-frequency detection pulses from the dc bias current. The voltage pulses generated from the SNSPD are amplified using a room-temperature 50 dB low-noise amplifier (RF Bay Inc. LNA-650) with the bandwidth from 30 kHz to 600 MHz. The amplified voltage pulses are then fed into a pulse counter and an oscilloscope. The system detection efficiency (SDE) is defined as $(\text{OPR}-\text{DCR})/\text{PR}$, where OPR is the output pulse rate of the SNSPD, measured with a photon counter, DCR is the dark count rate when the laser is blocked, and PR represents the total photon rate input to the system. Meanwhile, the SDE is the product of the on-chip detection efficiency (OCDE) and the photon loss (PL) during the transmission from the input fiber to the

NbN nanowire. In this setup, PL is composed of coupling loss of the grating coupler (GCL), the transmission loss in the waveguide (WL) and the split loss in the Y-junction ($Y_L=3$ dB). The transmission loss in the waveguide is negligible because of the short transmission distance of several hundreds of micrometers. The coupling loss of the grating coupler can be calibrated by measuring the loss between the two grating couplers (L_0). Thus $GCL=(L_0-YL)/2$, and $PL=GCL+YL=(L_0+YL)/2$. The OCDE of the device can be calculated by $\text{OCDE}=\text{SDE}/\text{PL}$.

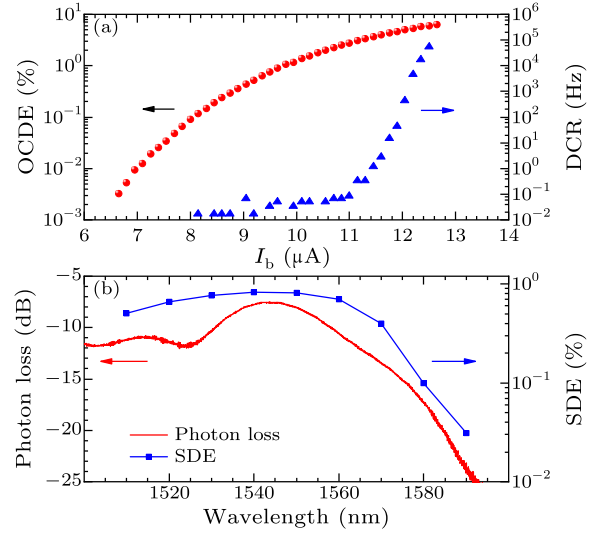


Fig. 3. (a) The OCDE and DCR of the detector. (b) The photon loss spectrum of the silicon waveguide part in the sample and SDE spectrum of the sample.

By measuring the loss between the two grating couplers, PL can be calculated to be 15.6% at wavelength 1550 nm, thus the OCDE can be calculated. Figure 3(a) presents the OCDE and DCR of the waveguide integrated SNSPD as a function of the bias current. The device shows 4% OCDE at DCR of 3 Hz. Owing to the polarization selectivity of the grating coupler, the device also has high polarization sensitivity to the incident light. The polarization extinction ratio (PER, the ratio of the maximum detection efficiency to the minimum detection efficiency) can reach more than 200, which indicates the great potential in the polarization-sensitive detection.

Figure 3(b) shows the spectral characteristic of the waveguide-integrated SNSPD. The red curve shows the photon loss spectrum, which is mainly shaped by the coupling spectrum of the grating coupler. The loss gets minimum at 1543 nm, and increases rapidly as the wavelength moves away. The blue line shows the measured SDE with the variation of the incident light wavelength, and its tendency is in good agreement with the photon loss spectrum.

Figure 4 shows the measured timing jitter of the device biased at $11.6 \mu\text{A}$ using the time-correlated single-photon counting (TCSPC) module with a resolution of 0.813 ps (SPC150). A 1550-nm-wavelength

pulsed laser with 100 fs pulse width and 20 MHz repetition rate is used. The measured timing jitter is 75 ps defined as the full width at half maximum (FWHM) of the histogram. The inset of Fig. 4 shows the averaged impulse waveform of the detector biased at $11.6 \mu\text{A}$ with a recovery time constant of 9.8 ns.

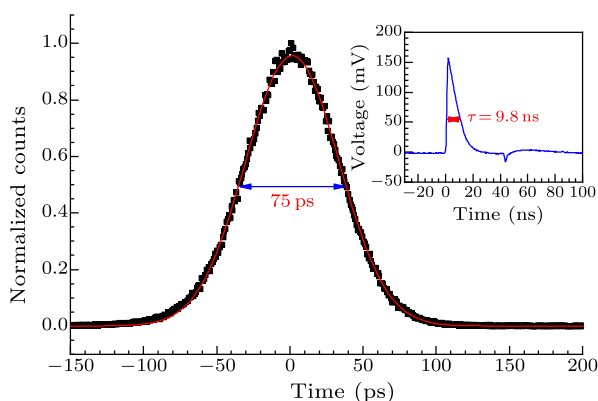


Fig. 4. Histogram during the timing jitter measurement. Inset: the averaged impulse waveform of the detector. The inset shows the averaged impulse waveform of the detector.

Though effective signal showing photon detection from a shallow-ridge silicon waveguide has been collected, the OCDE and the SDE of the detector are relatively low compared with the reported performance of Ref. [17]. Firstly, the unsaturation of the OCDE indicates that the intrinsic detection efficiency has not reached the unity. This may be due to the imperfect fabrication of the nanowire, which could be improved further. Secondly, with the temperature dropping to 2.1 K, the fiber may shift from the preset position, which would sharply decrease the coupling efficiency. With the low-temperature nano-positioners, the precise coupling can be realized at 2.1 K. Thirdly, the Y-junction for calibration introduces an extra 3 dB loss, which could be removed further. Finally, the current grating coupler design could realize 31.6% coupling efficiency at 1550 nm, which could be optimized further.[25]

In summary, a silicon shallow-ridge waveguide integrated superconducting nanowire single photon detector has been designed and fabricated. At the bias current of $11.6 \mu\text{A}$, 4% on-chip detection efficiency near 1550 nm wavelength is achieved with the dark count rate of 3 Hz. The measurement results demonstrate the feasibility of the integration of SNSPDs on silicon shallow-ridge waveguides, showing their potential on future quantum photonic circuits with a large-scale detector array.

Contributions: L. J. Yu and H. Q. Wang contributed equally to this work. L. J. Yu and H. Q. Wang designed the device. L. J. Yu fabricated the silicon photonic circuits on the device and measured

the optical performance of the chip, H. Q. Wang fabricated the SNSPD part on the device and measured the performance of the integrated SNSPD.

References

- [1] Chen T Y et al 2010 *Opt. Express* **18** 27217
- [2] Sun Q C et al 2016 *Nat. Photon.* **10** 671
- [3] Liao S K et al 2017 *Nature* **549** 43
- [4] Metcalf B J et al 2014 *Nat. Photon.* **8** 770
- [5] Xiong C et al 2015 *Optica* **2** 724
- [6] Santagati R, Silverstone J W, Strain M J, Sorel M, Miki S, Yamashita T, Fujiwara M, Sasaki M, Terai H, Tanner M G, Natarajan C M, Hadfield R H, O'Brien J L and Thompson M G 2017 *J. Opt.* **19** 114006
- [7] Paesani S, Ding Y, Santagati R, Chakhmakhchyan L, Vigliar C, Rottwitt K, Oxenløwe L K, Wang J, Thompson M G and Laing A 2018 *arXiv:1812.03158*[quant-ph]
- [8] Sibson P, Erven C, Godfrey M, Miki S, Yamashita T, Fujiwara M, Sasaki M, Terai H, Tanner M G, Natarajan C M, Hadfield R H, O'Brien J L and Thompson M G 2017 *Nat. Commun.* **8** 13984
- [9] Gol'tsman G N, Okunev O, Chulkova G, Lipatov A, Semenov A, Smirnov K, Voronov B, Dzardanov A, Williams C and Sobolewski R 2001 *Appl. Phys. Lett.* **79** 705
- [10] Marsili F, Verma V B, Stern J A, Harrington S, Lita A E, Gerrits T, Vayshenker I, Baek B, Shaw M D, Mirin R P and Nam S W 2013 *Nat. Photon.* **7** 210
- [11] Zhang W, You L, Li H, Huang J, Lv C, Zhang L, Liu X, Wu J, Wang Z and Xie X 2017 *Sci. Chin. Phys. Mech.* **60** 120314
- [12] Zadeh I E, Los J W N, Gourgues R B M, Steinmetz V, Bulgarini G, Dobrovolskiy S M, Zwiller V and Dorenbos S N 2017 *APL Photon.* **2** 111301
- [13] Zhang W J, Yang X Y, Li H, You L X, Lv C L, Zhang L, Zhang C J, Liu X Y, Wang Z and Xie X M 2018 *Supercond. Sci. Technol.* **31** 035012
- [14] Shibata H, Shimizu K, Takesue H and Tokura Y 2015 *Opt. Lett.* **40** 3428
- [15] Yang X Y, Li H, Zhang W J, You L X, Zhang L, Liu X Y, Wang Z, Peng W, Xie X M and Jiang M H 2014 *Opt. Express* **22** 16267
- [16] Sprengers J P, Gaggero A, Sahin D, Jahanmirinejad S, Frucci G, Mattioli F, Leoni R, Beetz J, Lermer M, Kamp M, Höfling S, Sanjines R and Fiore A 2011 *Appl. Phys. Lett.* **99** 181110
- [17] Pernice W H, Schuck C, Minaeva O, Li M, Goltzman G N, Sergienko A V and Tang H X 2012 *Nat. Commun.* **3** 1325
- [18] Kahl O, Ferrari S, Kovalyuk V, Goltzman G N, Korneev A and Pernice W H P 2015 *Sci. Rep.* **5** 10941
- [19] Rath P, Kahl O, Ferrari S, Sproll F, Lewes-Malandrakis G, Brink D, Ilin K, Siegel M, Nebel C and Pernice W 2015 *Light: Sci. Appl.* **4** e338
- [20] Schuck C, Guo X, Fan L, Ma X, Poot M and Tang H X 2016 *Nat. Commun.* **7** 10352
- [21] Sibson P, Kennard J E, Stanicic S, Erven C, O'Brien J L and Thompson M G 2017 *Optica* **4** 172
- [22] Vlasov Y A and McNab S J 2004 *Opt. Express* **12** 1622
- [23] Dong P, Qian W, Liao S, Liang H, Kung C C, Feng N N, Shafiha R, Fong J, Feng D and Krishnamoorthy A V 2010 *Opt. Express* **18** 14474
- [24] Annunziata A J, Quaranta O, Santavica D F, Casaburi A, Frunzio L, Ejrnaes M, Rooks M J, Cristiano R, Pagano S, Frydman A and Prober D E 2010 *J. Appl. Phys.* **108** 084507
- [25] Zhang C, Sun J H, Xiao X, Sun W M, Zhang X J, Chu T, Yu J Z and Yu Y D 2013 *Chin. Phys. Lett.* **30** 014207